Sperm-templated magnetic microrobots

Veronika Magdanz[1]*, Johannes Gebauer[1], Dalia Mahdy[2], Juliane Simmchen[3], Islam S.M. Khalil[4]

***Abstract*— Spermatozoa are efficient microswimmers which perform a bending wave motion for their forward propulsion. By binding positively charged iron oxide microparticles to the surface of negatively charged bull spermatozoa, we fabricate sperm-templated biohybrid magnetic microrobots. This study presents an easy and cost-efficient method to obtain magnetic microswimmers that are actuated by oscillating magnetic fields and take advantage of the intrinsic flexibility of the sperm tails for their propulsion in fluidic environment. In this article, we present the actuation of such sperm-templated flexible magnetic microsrobots under influence of an oscillating magnetic field and investigate their performance on the solid-liquid and liquid-gas interface.**

I. Introduction

Numerous biomedical science areas have benefited from the interaction of cells and magnetic nanoparticles for applications in nanomedicine, imaging, actuation and more. Especially in the development of artificial and bio-hybrid microswimmers, magnetic particles have been important constituents from the very beginning [1]. Mostly used for the facile addition of magnetic property useful for actuation, magnetic micro-and nanoparticles offer further functionality, for instance as contrast agents in ultrasound imaging or magnetic resonance imaging. Several approaches have been undertaken to fabricate bio-hybrid magnetic swimmers. In particular, helical microstructures found plentiful in nature are an attractive source of designing shapes that are advantageous for efficient propulsion on the microscale. For instance, plant-based helical swimmers were fabricated by depositing magnetic layers onto spiral xylem vessel plant fibers [2].

Also bacteria display helical structures, so Kamata *et al*. have developed *Spirulina*-templated microcoils by adding a metal coating to *Spirulina*. The *Spirulina*-templated microcoils are developed by generating a thin metal layer on the Spirulina via electroless plating [3]. Li *et al*. have also investigated the behavior of *Spirulina*-templated microcoils in alternating electric fields, and demonstrated directional control using different configuration of actuating electrodes[4]. Yan *et al*. have used a dip-coating process in magnetite suspensions to fabricate helical microswimmers from *Spirulina* microalgae. In addition, *in vivo* magnetic resonance imaging of the microswimmer has been achieved inside a rodent stomach [5]. However, these bio-templated magnetic swimmers all display rigid properties and propel in a helical motion, similar to a corkscrew-motion, which has been thoroughly explored using fully artificial structures from the micro- to the nanoscale.[6,7,8] Inspired by sperm cells, several soft magnetic microrobots have been developed and locomotion has been achieved in low Reynolds numbers by a traveling wave to generate propulsion. Dreyfus *et al.* have developed a soft microrobot using a chain of colloidal magnetic particles linked by DNA and attached to a red blood cell[1]. The actuation of this microrobot has been demonstrated using external magnetic fields by generating a planar traveling wave along the linked chain of particles. Jang *et al.* have also demonstrated planar flagellar propulsion of composite multilink nanowire-based chains[9]. Closed-loop control of artificial soft microrobots[10], controllable motion of microrobots along narrow channels with bifurcations[11], and controllable transitions between planar-to-helical flagellar propulsion [12] have been also demonstrated owing to their flexibility. Spermatozoa have previously been proposed as components of microrobots, as power sources for the propulsion of microtubes or as functional components towards applications in assisted reproduction technology.[13]–[15]

Here, we use an electrostatically driven self-assembly process to bind positively charged magnetic microparticles on the whole cell surface of non-motile bovine spermatozoa (see schematic in Figure 1a). These particle-cell hybrids are

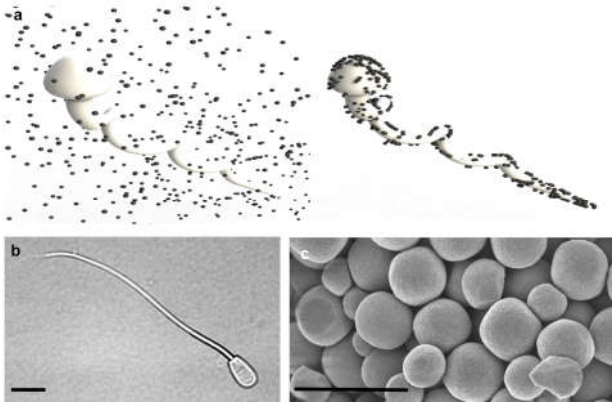

Figure 1: a) Scheme of bovine spermatozoa in particle suspension and fully covered with 1 µm iron oxide particles. b) Bright field microscopic image of a single sperm cell. Scale bar 10 µm. c) SEM image of Fe_2O_3 particles. Scale bar 2 µm.

*Research supported by the Excellence initiative of the TU Dresden.

Author information

[1] V. Magdanz and J. Gebauer are affiliated with the Chair of Applied Zoology, TU Dresden, Zellescher Weg 20, 01062 Germany. e-mail: veronika.magdanz@tu-dresden.de

[2]D. Mahdy is affiliated with the Mechatronics Department, the German University in Cairo, New Cairo 11835, Egypt.

[3] J. Simmchen is affiliated with Physical Chemistry, TU Dresden, Zellescher Weg 19, 01062 Dresden, Germany

[4]I. S. M. Khalil is affiliated with the Biomechanical Engineering Department, University of Twente, 7522 NB Enschede, The Netherlands.

Acknowledgments: V.M. thanks Dr. D. Voigt for assistance with cryoSEM and C. Ridzewski for support in video recording and analysis. V.M. and J.G. thank the Faculty of Biology, Alex Froschauer and Klaus Reinhardt for providing lab space and access to equipment. J.S. acknowledges a Freigeist fellowship from the Volkswagen foundation (grant number 91619).

978-1-7281-0948-0/19/$31.00 ©2019 IEEE

actuated in an oscillating magnetic field and display forward motion.

With this self-assembly approach, even more so than with traditional fabrication techniques of soft microrobots, we preserve the optimal geometry of sperm cells and their organic bodies. The former is essential for optimal locomotion, while the later provides an organic host for drug delivery and several biomedical applications.

I. Materials & Methods

A. Preparation of sperm-particle constructs

Cryo-preserved bovine semen was purchased from Masterrind GmbH and kept in liquid nitrogen storage until use. Bovine semen straws were thawed in a 38°C water bath for 2 minutes, resuspended in 1mL SP-TALP (Caisson Lab, modified tyrode's albumin lactate pyruvate medium) and centrifuged at 300g for 5 minutes in no-brake mode. The supernatant was removed and the sperm pellet was then resuspended in 1 mL deionized water and centrifuged again at 300g for 5 minutes. A single bovine sperm cell is displayed in Figure 1b. The supernatant was removed and an aqueous suspension of 1 µm iron oxide particles was used to resuspend the sperm. The sperm were incubated with the iron oxide particles for 24h at room temperature before use. It should be noted that due to the incubation of the bull sperm with particles in deionized water for 24 hours, the spermatozoa were not motile anymore.

B. Magnetic control setup

An electromagnetic system with four orthogonal electromagnetic coils was used to actuate the sperm-templated magnetic microrobots. Each coil has an inner- and outer diameter of 20 mm and 40 mm, respectively. The length and number of turns of each coils are 80 mm and 3200 turns, respectively, and the thickness of the wire is 0.7 mm. The samples were contained inside a reservoir in the common center of the electromagnetic coils. At this point, the magnetic field and the field gradient were measured as ~20 mT and ~5 T/m, respectively. The magnetic torque exerted on the magnetic dipole of the microrobots enables directional control that is observed using microscopic feedback.

The magnetic particles are magnetized prior to actuation by the electromagnetic coils, so that they provide a magnetic dipole moment approximately along the propulsion axis of the cell.

C. Magnetic actuation

The four electromagnetic coils were independently supplied with current inputs using electric drivers (MD10C, Cytron Technologies Sdn. Bhd, Kuala Lumpur, Malaysia) and controlled via a control board (Arduino Uno Rev3). Matlab routine is developed for teleoperation with an Extreme 3D pro Joystick (963290-0403, Logitech, Newark, USA) using microscopic feedback.

D. cryoSEM

The cryo-(FE-)SEM SUPRA 40VP-31-79 (Carl Zeiss SMT Ltd., Oberkochen, Germany) equipped with an EMITECH K250X cryo-preparation unit (Quorum Technologies Ltd., Ashford, Kent, United Kingdom) was used for imaging of the sperm-particle constructs. 2 µL of suspension was dropped onto a glass slide fixed to the cryo-SEM holder and immediately shock-frozen in liquid nitrogen in the slushing chamber. From there it was transferred to the cryo preparation chamber at -140 °C, sublimed for 10-15 minutes at -70 °C, and sputter coated with platinum (layer thickness ca. 6 nm). Subsequently, it was transferred to the SEM, and then examined in a frozen state at 5 kV accelerating voltage and -100 °C temperature using the secondary electron (SE) detector.

E. Video recording and analysis

Sperm-particle constructs were imaged under a Leica Wild M3Z stereomicroscope with a custom-built TV-adapter (3x, Thalheim Special Optik, see Figure 2) and recorded with a Basler camera acA1300_200uc and pylon viewer software at 30 frames per second. A controlled magnetic field is applied on the samples to exert magnetic torque on the sperm.

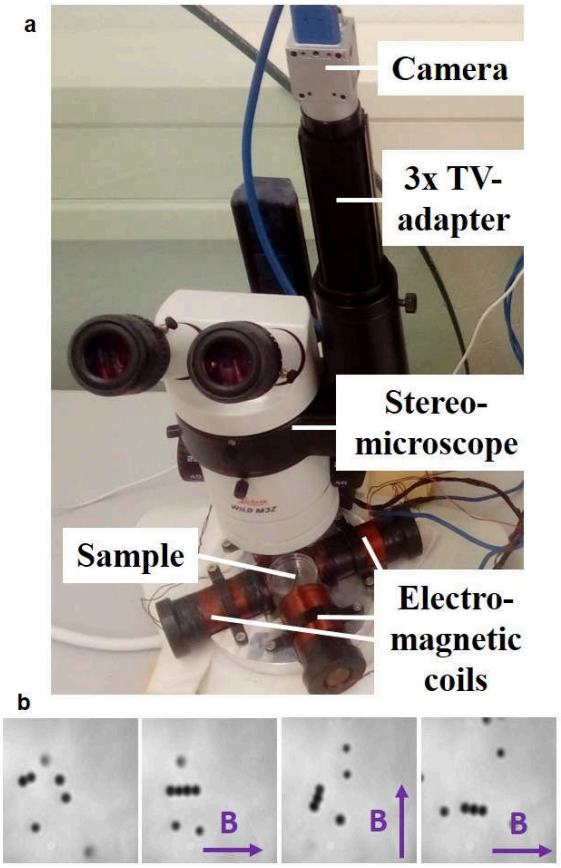

Figure 2: a)Custom-made experimental setup with four Helmholtz coils located around the sample and stereomicroscope with camera. b) Reaction of iron oxide particles to the magnetic field.

F. Synthesis of magnetic particles

90 ml of 6M NaOH solution was added quickly to 100ml of 2M $FeCl_3*6H_2O$ solution, the solution was stirred for 10 min and 10 ml of MiliQ water were added. The resulting mixture was added into a pyrex bottle and left for 10 days at 100°C. The product was washed several times with ethanol and water and subsequently characterized by dynamic light scattering (particle size 888±45 nm) with a poly dispersity index of 0.227.

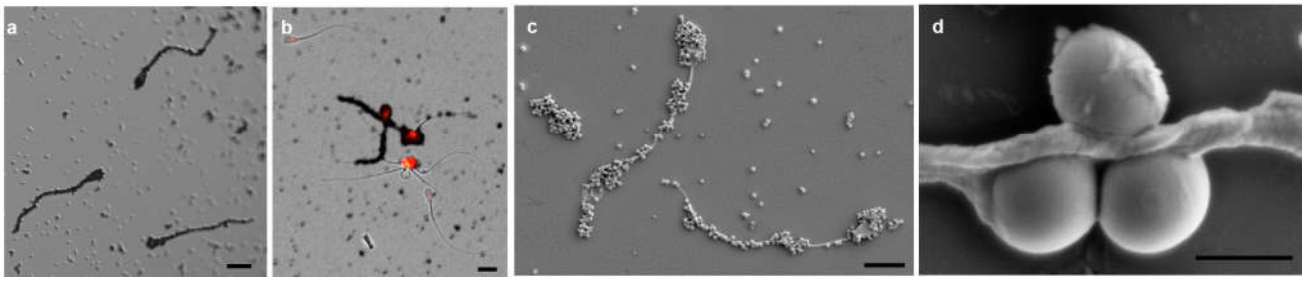

Figure 3: Characterization of sperm-particle assemblies: a) bright field image of particle-sperm assemblies. b) Superimposed bright field/fluorescent image of spermatozoa with magnetic particles stained with Live/Dead kit SYBR14 (green cells=alive) and propidium iodide (red = dead cells). The live/dead stain indicates that all spermatozoa are dead after assembly with microparticles in deionized water for 24h (dead cells are stained read). Scale bar 10µm. c) cryoSEM image. Scale bar 10 µm. d) cryoSEM image of iron oxide particles on bovine sperm flagellum. Scale bar 1 µm.

II. Results

First, we investigated the interaction of bovine spermatozoa with 1 µm iron oxide particles. Bovine spermatozoa are 60 – 70 µm long, including a 10 µm long, 5 µm wide, 1 µm thick head and a tail that is 50-60 µm long and 1 µm thick with slightly decreasing thickness towards its distal end (see Figure 1b). The 1 µm large particles consist of Fe_2O_3 and display a surface zeta potential of +46 mV in water, while sperm cells are negatively charged.[16] To confirm the negative surface charge of the spermatozoa, we compared two different measurement principles to conclude on the surface conditions. Firstly, using the standard Zetasizer (Malvern) in strongly diluted sperm medium, we achieved an average value of -28mV. However, since the size and shape of sperm cells is far from ideal for dynamic light scattering, we confirmed this value in a home-made microelectrophoresis setup, where we placed a solution of sperm cells in a defined cell between two electrodes, applying a voltage. After establishing the electric field, we observed the migration of non-motile sperm cells towards the positively charged electrode, resulting in an electric mobility in the same order (about -15 mV). The adhesion between the particles and sperm cells was studied as described in the following section.

A. *Assembly process of sperm-templated microrobots*

It was found that the magnetic particles attach to the whole surface of bovine spermatozoa without surface functionalization (see Figure 3) or any directed assembly steps, simple incubation was sufficient. We assume that the interaction is based on electrostatic interactions, because sperm cells are negatively charged[16] and the magnetic particles have a positive surface charge. The sperm-particle constructs are stable for up to several weeks in water or in buffered sperm medium containing bovine serum albumin, lactate and pyruvate when kept in the fridge. In the next step, we demonstrate the potential for using non-motile spermatozoa as biological templates for the cheap production of magnetically driven flexible microrobots without the need of deposition devices. Positively charged particles attach to the whole body of dead sperm cells (see Figure 3) and thus allow magnetic actuation of the sperm-particle constructs. The sperm cells used for the actuation were completely covered by the iron oxide particles (see Figure 3a and 3c). From scanning electron microscopy, it can be observed that, per single spermatozoon, on average, more than 100 microparticles are attached. Live/dead stain of the spermatozoa confirmed that all spermatozoa were dead after 24h incubation in deionized water (Figure 3b).

B. *Magnetic actuation of sperm-templated microrobots*

Before actuating the assemblies, we checked the responsiveness of the iron oxide particles in a magnetic field. Therefore, similarly to the assemblies, the particles were magnetized on a strong permanent magnet and then introduced into a dynamic magnetic field. Initially, particles form lines, which then reorient after switching the field. If the field is applied, these lines do not fall apart after removing the applied field and can be turned (see Fig. 2b). For individual particles, no reorientation is visible, which could be due to their spherical morphology.

The actuation was performed with a magnetic control setup consisting of 4 orthogonal electromagnetic coils. After the assembly, we performed the magnetization of the sperm-particle-assemblies with a strong permanent magnet. Given a particle size of about 1 µm the particles definitely contain magnetic domains, but the magnetic field in the coils is not strong enough to re-magnetize the particles. Once magnetized, the sperm-templated magnetic microrobots are contained in the common center of the electromagnetic coils. Uniform magnetic fields are applied along the direction of propulsion with sinusoidally varying orthogonal component to induce bending wave along the flexible flagellum of the microrobots. The magnetic microparticles provide a magnetization along the long axis of the sperm cell. Therefore, the external magnetic field exerts a magnetic torque on the dipole of the microswimmer, and achieves directional control along the field lines.

We recorded the actuated sperm-templated microrobots over a range of frequencies (1-20Hz) in order to test their performance in different frequencies and explore their forward propulsion.

We noticed considerably different motion behavior between sperm-templated microrobots that were located on the bottom of the petri dish compared to the microswimmers on the air-liquid interface. Therefore, we studied their performance depending on their location (solid-liquid interface on the bottom of the petri dish) versus liquid-air-interface on the top of the medium.

- *Rolling swimmers at the solid-liquid interface*

Before turning on any magnetic field, the particle-sperm constructs lie immotile in close vicinity of the glass substrate. Due to the size of the assembly only little Brownian motion is expected, but the attractive interactions between the positive iron oxide parts and the negatively charged glass lessen the random motion further. No convective effects are observed. Figure 5 and videos S1 and S2 illustrate the motion of the sperm-templated microrobots on the bottom of the petri dish under the influence of the magnetic field with a frequency of

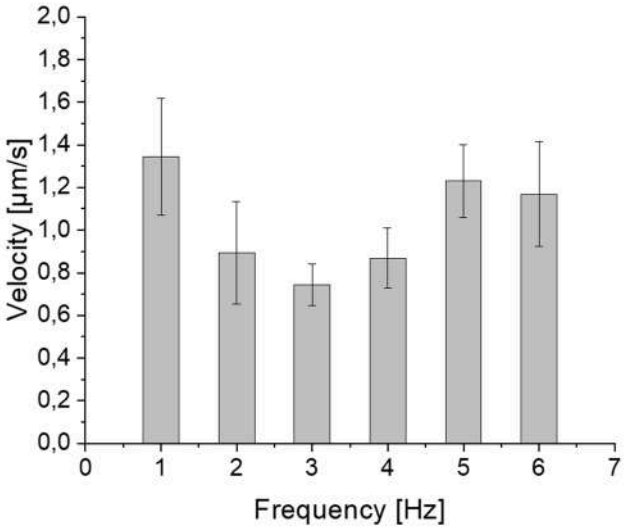

Figure 4: Average velocities sperm-templated microrobots actuated on solid-liquid interface. Error bars are standard error (N>8 for each bar).

1 Hz and 3 Hz, respectively. After mixing the sperm-particle constructs in a petridish with 1 mL water, most sperm-templated microrobots accumulate on the bottom of the dish, due to their density mismatch with the surrounding media.

The sperm-templated microrobots perform a rolling motion on the solid-liquid interface, which is governed by strong drag forces or attractive interactions with the surface.

Thus, the average velocities of the sperm-templated microrobots are low (around 1 µm/s) across the whole range of tested frequencies. At frequencies above 6 Hz, more and more sperm-templated swimmers cannot follow the magnetic actuation due to the step-out frequency. It is known that microrobots need to follow synchronously the applied field for optimum propulsion. If the step-out frequency is exceeded, the velocity rapidly declines.[17] For this reason, we did not include these data in Figure 4 and 6.

The resulting average velocities are displayed in Figure 4. The forward velocity seems highest at 1 Hz, but there is no significant change when increasing the frequency.

An image series in Figure 5 (and videos S1 and S2) illustrates the rolling forward motion of the sperm-templated microrobots on the solid-liquid interface, and also a slight bending of the sperm body can be clearly observed. It is visible that the forward motion does not occur head first, but sideways or tail first.

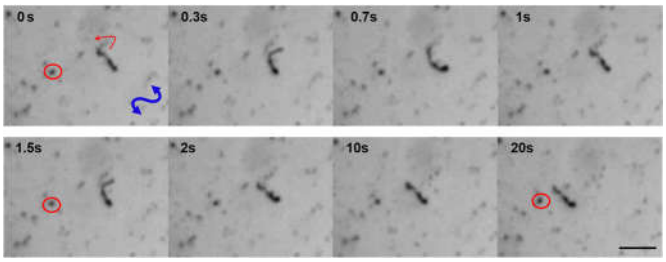

Figure 5: Image series over a time span of 20 seconds of a sperm-templated microrobot at an applied rolling over the bottom surface of the petri dish. The red circle marks a reference point. The blue arrow marks the applied orthogonal sinusoidal magnetic field. Scale bar is 50 µm.

- *Air-liquid interface microrobots*

When mixing the sperm-particle constructs in the petridish with water, some sperm-templated microrobots remain on the air-liquid interface due to the relatively high surface tension in water (no surfactants are used here). Here, even without magnetic field some convective influences can be observed. In a video documentation these would show as movement within the field of view, but not relative to objects that are also pinned to the air-liquid interface. In contrast to the rolling swimmers on the bottom of the petridish, the sperm-templated microrobots on the air-liquid interface, achieve much higher average velocities, see video S3 and video S4, which were actuated at 1 Hz and 3 Hz, respectively (convective effects not taken into account).

The average velocities depending on the frequency are displayed in Figure 6. It is shown that the average velocities of the air-liquid interface magnetic microrobots are about 10 times higher (8-15 µm/s).

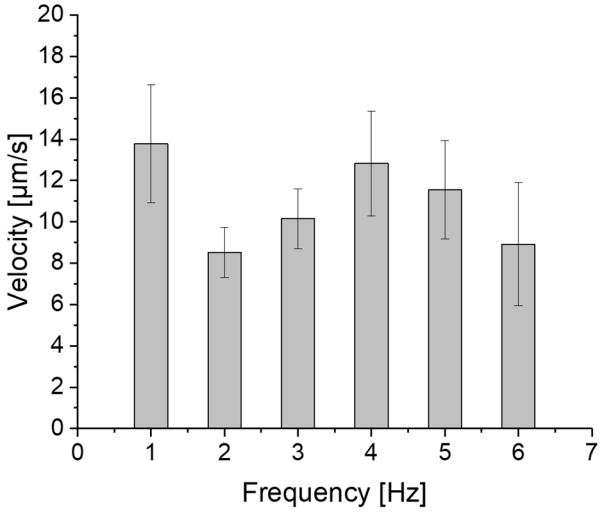

Figure 6: Average velocities sperm-templated microrobots actuated on air-liquid interface. Error bars are standard error (N>6 for each bar).

The image series in Figure 7 illustrates the motion of the sperm-templated microrobots at the air-liquid interface. Here, the swimmers move head first and much faster than the sperm-templated microrobots on the bottom of the petridish. They also follow the magnetic actuation much stronger (compare Figure 5 versus Figure 7).

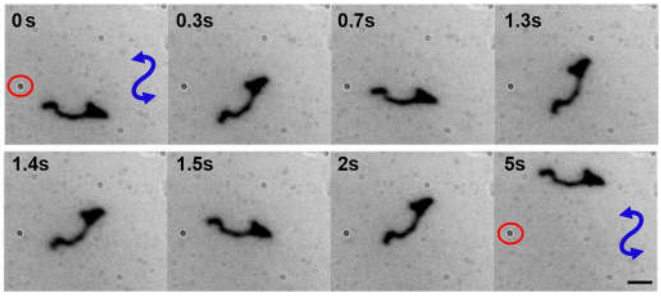

Figure 7: Image series of sperm-templated microrobot at the air-liquid interface over the range of 5 seconds actuated with 1 Hz. The red circle marks a reference particle which is not moving. The blue arrow displays the applied orthogonal sinusoidal magnetic field. Scale bar is 10 µm.

III. Conclusions

We demonstrate the actuation of non-motile spermatozoa by attaching magnetic microparticles and application of a rotating magnetic field. The sperm-particle binding is based on electrostatic interactions and therefore are a straightforward method to add magnetic properties to the sperm cells without any engineering techniques of chemical surface functionalization. We observed, that in both cases (on the substrate, as well as on the air-liquid interface) the frequency that results in the highest forward speed is rather low (1Hz, see Figure 4 and 6). The sperm-templated magnetic microswimmers are stable in aqueous solutions (water and sperm medium SP-TALP (modified tyrode's albumin lactate pyruvate medium)) for several weeks at 4°C. The actuation of the flexible microswimmers was performed under room temperature, but there is no doubt that they can also function under physiological temperature.

In contrast, comparing the forward motion to the natural beating frequency of the motile bull sperm, we see that the biological part can achieve much faster oscillations (in the order of 5-15 Hz[18]), which results in much higher swimming velocities (ca. 100 µm/s). This shows that from the material point of view, there is potential for improvement in the actuation of these sperm-templated magnetic microrobots. In our observations, the flexibility of the tail is not fully explored yet and most of the microrobots act as rather rigid swimmers. The rolling swimmers on the solid-liquid interface display bending motion more frequently which is probably due to attraction effects or interactions with the surface, as mentioned before. This indicates that the magnetic actuation alone is not able to fully employ the bending motion of the sperm-templated microrobots. In larger structures such as the artificial soft robotic sperm[12], this has previously been achieved. It would be interesting to find out under which conditions these sperm-templated microrobots act as flexible microrobots, using the biologically intrinsic flexibility of tail. One possible approach might be the use of colloid supported lipid bilayers which enable the assembly of flexible structures.[19]

Additionally, different particle configurations need to be explored in future experiments. Depending on the size, shape, surface and magnetization, the resulting performance of the sperm-templated microrobots might be improved. The particle attachment distribution to the head, midpiece and tail of the spermatozoa will also be taken into consideration in future investigations. Different configurations of the magnetic field might also give better forward propulsion. It will be interesting in future studies to explore the actuation in media with higher viscosities and with obstacles in order to mimic the natural environment of spermatozoa. Apart from the straightforward fabrication method of the magnetic microrobot by sperm cells as templates, they also hold potential as carriers. As recently was demonstrated, sperm cells can be loaded with surprisingly high amounts of cancer drug,[20] dead sperm cells could be used as carriers for various cargo.

References

[1] R. Dreyfus, J. Baudry, M. L. Roper, M. Fermigier, H. A. Stone, and J. Bibette, "Microscopic artificial swimmers," *Nature*, vol. 437, no. 7060, pp. 862–865, Oct. 2005.

[2] W. Gao *et al.*, "Bioinspired Helical Microswimmers Based on Vascular Plants," *Nano Lett.*, vol. 14, no. 1, pp. 305–310, Jan. 2014.

[3] K. Kamata *et al.*, "Spirulina-Templated Metal Microcoils with Controlled Helical Structures for THz Electromagnetic Responses," *Sci. Rep.*, vol. 4, no. 1, p. 4919, May 2015.

[4] X. Li, J. Cai, L. Sun, Y. Yue, and D. Zhang, "Manipulation and assembly behavior of Spirulina-templated microcoils in the electric field," *RSC Adv.*, vol. 6, no. 80, pp. 76716–76723, Aug. 2016.

[5] X. Yan *et al.*, "Multifunctional biohybrid magnetite microrobots for imaging-guided therapy," *Sci. Robot.*, vol. 2, no. 12, p. eaaq1155, Nov. 2017.

[6] D. Walker, M. Kübler, K. I. Morozov, P. Fischer, and A. M. Leshansky, "Optimal Length of Low Reynolds Number Nanopropellers," *Nano Lett.*, vol. 15, no. 7, pp. 4412–4416, Jul. 2015.

[7] A. Ghosh and P. Fischer, "Controlled Propulsion of Artificial Magnetic Nanostructured Propellers," *Nano Lett.*, vol. 9, no. 6, pp. 2243–2245, Jun. 2009.

[8] D. J. Bell, S. Leutenegger, K. M. Hammar, L. X. Dong, and B. J. Nelson, "Flagella-like propulsion for microrobots using a nanocoil and a rotating electromagnetic field," in *Robotics and Automation, 2007 IEEE International Conference on*, 2007, pp. 1128–1133.

[9] B. Jang *et al.*, "Undulatory locomotion of magnetic multilink nanoswimmers," *Nano Lett.*, vol. 15, no. 7, pp. 4829–4833, 2015.

[10] I. S. M. Khalil, H. C. Dijkslag, L. Abelmann, and S. Misra, "MagnetoSperm: A microrobot that navigates using weak magnetic fields," *Appl. Phys. Lett.*, vol. 104, no. 22, p. 223701, 2014.

[11] I. S. M. Khalil, M. Hafez, A. Klingnert, S. Scheggi, B. Adel, and S. Misra, "Near Surface Effects on the Flagellar Propulsion of Soft Robotic Sperms," in *2018 7th IEEE International Conference on Biomedical Robotics and Biomechatronics (Biorob)*, 2018, pp. 384–389.

[12] I. S. M. Khalil, A. F. Tabak, M. A. Seif, A. Klingner, and M. Sitti, "Controllable switching between planar and helical flagellar swimming of a soft robotic sperm," *PLoS One*, vol. 13, no. 11, p. e0206456,

2018.
[13] V. Magdanz, S. Sanchez, and O. G. Schmidt, “Development of a Sperm-Flagella Driven Micro-Bio-Robot,” *Adv. Mater.*, vol. 25, no. 45, pp. 6581–6588, 2013.
[14] V. Magdanz, M. Medina-Sánchez, L. Schwarz, H. Xu, J. Elgeti, and O. G. Schmidt, “Spermatozoa as Functional Components of Robotic Microswimmers,” *Adv. Mater.*, vol. 29, no. 24, p. 1606301--n/a, 2017.
[15] M. Medina-Sánchez, L. Schwarz, A. K. Meyer, F. Hebenstreit, and O. G. Schmidt, “Cellular cargo delivery: Toward assisted fertilization by sperm-carrying micromotors,” *Nano Lett.*, vol. 16, no. 1, pp. 555–561, 2015.
[16] R. Yanagimachi, Y. D. Noda, M. Fujimoto, and G. L. Nicolson, “The distribution of negative surface charges on mammalian spermatozoa,” *Am. J. Anat.*, vol. 135, no. 4, pp. 497–519, 1972.
[17] A. W. Mahoney, N. D. Nelson, K. E. Peyer, B. J. Nelson, and J. J. Abbott, “Behavior of rotating magnetic microrobots above the step-out frequency with application to control of multi-microrobot systems,” *Appl. Phys. Lett.*, vol. 104, no. 14, p. 144101, Apr. 2014.
[18] R. Rikmenspoel, “Movements and active moments of bull sperm flagella as a function of temperature and viscosity.,” *J. Exp. Biol.*, vol. 108, no. 1, pp. 205–230, 1984.
[19] M. Rinaldin, R. W. Verweij, I. Chakraborty, and D. J. Kraft, “Colloid supported lipid bilayers for self-assembly,” *Soft Matter*, vol. 15, no. 6, pp. 1345–1360, 2019.
[20] H. Xu, M. Medina-Sánchez, V. Magdanz, L. Schwarz, F. Hebenstreit, and O. G. Schmidt, “Sperm-Hybrid Micromotor for Targeted Drug Delivery,” *ACS Nano*, Dec. 2017.